

Article

# Activated Carbons as Methanol Adsorbents for a New Cycle “Heat from Cold”

Ilya Girnik \*, Alexandra Grekova, Larisa Gordeeva and Yuri Aristov 

Boreskov Institute of Catalysis, Ac. Lavrentiev av. 5, 630055 Novosibirsk, Russia; grekova@catalysis.ru (A.G.); gordeeva@catalysis.ru (L.G.); aristov@catalysis.ru (Y.A.)

\* Correspondence: girnik@catalysis.ru; Tel.: +7-383-326-9454

Received: 26 June 2020; Accepted: 6 August 2020; Published: 8 August 2020



**Abstract:** Activated carbons are widely used for sustainable technology of adsorptive transformation and storage of heat. Here, we analyze the applicability of twelve commercial carbons and an innovative carbonaceous composite “LiCl confined to multi-wall carbon nanotubes” (LiCl/MWCNT) for a new cycle “Heat from Cold” (HeCol). It has recently been proposed for amplification of low-temperature ambient heat in cold countries. The analysis is made in terms of the methanol mass exchanged and the useful heat generated per cycle; the latter is the main performance indicator of HeCol cycles. The maximum specific useful heat, reaching 990 and 1750 J/g, can be obtained by using carbon Maxsorb III and the composite, respectively. For these materials, methanol adsorption dynamics under typical HeCol conditions are experimentally studied by the large pressure jump method. Before making this analysis, the fine carbon powder is consolidated by either using a binder or just pressing to obtain larger particles (ca. 2 mm). The methanol desorption from the consolidated samples of Maxsorb III at  $T = 2\text{ }^{\circ}\text{C}$  is faster than for LiCl/MWCNT, and the maximum (initial) useful power reaches (2.5–4.0) kW/kg sorbent. It is very promising for designing compact HeCol units utilizing the carbon Maxsorb III.

**Keywords:** adsorptive heating; methanol; activated carbons; useful heat; adsorption dynamics

## 1. Introduction

Porous carbonaceous materials have been known about since earliest times, e.g., the Egyptians and Sumerians used wood chars in medicine [1], water purification and the manufacture of bronze [2]. Nowadays, an enormous variety of activated carbons (ACs) are available in grains, extrudates, monolith, fibers, cloths, etc. [2–4]. Commercial ACs are widely used in various adsorption technologies because they are produced at a large scale and have a high adsorption capacity. In particular, ACs were proposed for adsorptive heat transformation and storage (AHTS) [5–8], which is an emerging sustainable technology to utilize low-temperature heat. This heat is readily available from renewable sources, such as solar energy, and heat wasted from industry, transport, dwellings, etc. A novel cycle “Heat from Cold” (HeCol) was proposed for amplification of low temperature ambient heat in cold countries [9].

The HeCol cycle uses the heat of a natural non-frozen water basin (e.g., river, lake, groundwater, sea, etc.) with the temperature  $T_M = 0\text{--}20\text{ }^{\circ}\text{C}$  as a heat source for evaporation and the adsorbent regeneration. The ambient air with a low temperature  $T_L$  from  $-50$  to  $-20\text{ }^{\circ}\text{C}$  serves as a sink for condensation heat. The useful heat is generated at the temperature  $T_H > 30\text{--}35\text{ }^{\circ}\text{C}$ , sufficient, e.g., for floor heating in dwellings. The 3T working cycles consists of two isosteres (1–2 and 3–4 in Figure 1) and two isotherms (2–3 and 4–1). The HeCol cycle is realized as follows: the adsorbent with the minimum uptake  $w_1$  is isosterically heated from  $T_M$  to  $T_H$  (line 1–2), then the adsorber is connected to the evaporator maintained at  $T_M$ . A jump in adsorptive pressure over the adsorbent initiates the isothermal adsorption process (2–3). The released adsorption heat  $Q_{\text{ads}}$  is transferred to a consumer

at  $T_H$ , while the heat  $Q_{ev}$  for evaporation is consumed for free from the ambient heat source at  $T_M$ . When the adsorbent is saturated by adsorptive to the maximum uptake  $w_2$ , the adsorber is disconnected from the evaporator and isosterically cooled down to the medium temperature  $T_M$  (line 3–4). Then, the adsorber is connected to the condenser at the low temperature  $T_L$ . The pressure drops to  $P_L$ , triggering desorption at  $T_M$ . The heat for desorption  $Q_{des}$  is supplied from the natural water basin at  $T_M$  and the condensation heat  $Q_{con}$  is dissipated to the ambient air at  $T_L$ .

Thus, the heat of non-frozen water basin at  $T_M$  is transformed into the useful heat  $Q_{us}$  at  $T_H$ , and the rest is refused to the ambient at  $T_L$ . Since the heat sink with low temperature is a prerequisite for the cycle operation, it was called “Heat from Cold”.

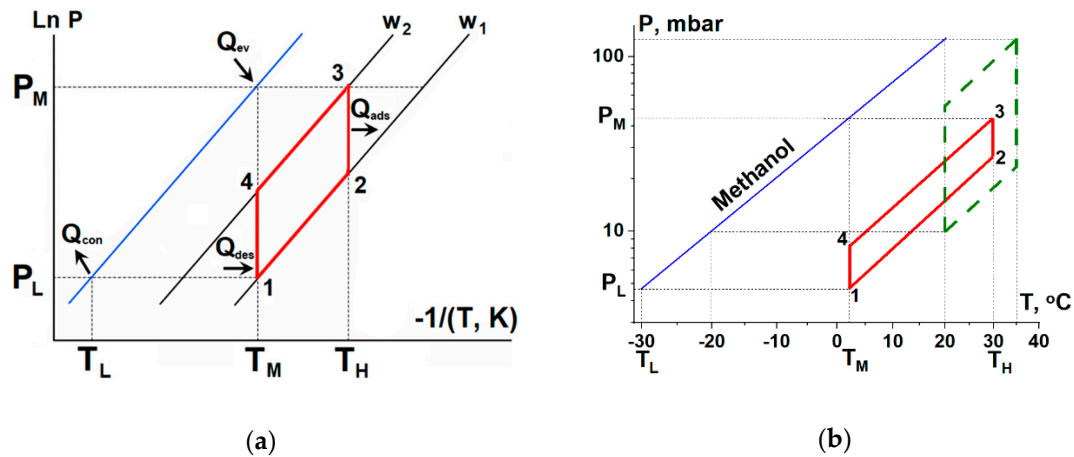


**Figure 1.** *P-T* diagrams of 3T HeCol working cycles: (a)—general one and (b)—for the “Maxsorb III—methanol” working pair (dashed line—cycle 1, solid line—cycle 2; see the text).

For the first theoretical [10,11] and experimental [12–15] studies of the HeCol cycle, methanol was used as an adsorptive because of its low freezing temperature ( $-97.6\text{ }^\circ\text{C}$ ). It always remains liquid under any conditions of the HeCol cycle. A commercial carbon ACM-35.4 was tested as an adsorbent, as it had been successfully used in AHTS processes [4,16]. In addition, it is available and cheap. These studies demonstrated that the HeCol cycle is feasible, and the temperature level of the useful heat can be sufficient for floor heating in low-energy buildings. A quite large specific power obtained in the first HeCol prototype (8.6 kW/kg-carbon) indicated quite fast methanol adsorption on this carbon. However, the specific useful heat  $Q_{us}$  reachable by using the working pair “methanol—AMC-35.4” does not exceed 235 J/g-carbon (for the cycle with boundary temperatures  $T_L/T_M/T_H = -20/20/35\text{ }^\circ\text{C}$ ). This could be mostly due to the relatively small specific mass of methanol exchanged in the cycle ( $\Delta w = 0.24\text{ g/g-carbon}$ ). This mass corresponds well to the equilibrium methanol exchange for the studied carbon [12]. At the lower temperature of the heat source for desorption ( $T_L/T_M/T_H = -30/2/30\text{ }^\circ\text{C}$ ), the useful heat dramatically drops to 70 J/g-carbon. This is due to reducing the amount of methanol exchanged to  $\Delta w = 0.08\text{ g/g-carbon}$  [12]. Such a modest useful heat leads to the enhanced size of HeCol units, which, in its turn, increases the inert thermal mass of the unit and further reduces the  $Q_{us}$ -value. Therefore, carbons with advanced methanol exchange in the HeCol cycle are highly desirable.

In this work, we make a comparative thermodynamic analysis of various commercial carbons as methanol adsorbents, keeping in mind the application in the HeCol cycles (Section 3). An innovative composite “LiCl confined to multi-wall carbon nanotubes” (LiCl/MWCNT) [17] is also briefly considered and compared with pure carbons because of its high methanol sorption capacity. This sorbent appears to be very promising for many AHTS applications in various climates [18]. Carbon Maxsorb III [19] is found to possess the largest methanol uptake variation under conditions of the HeCol cycle among the ACs studied. As it ensures the best performance of the cycle, it is chosen for studying methanol adsorption dynamics (Section 4). Its isothermal dynamics is compared with that on ACM-35.4 and LiCl/MWCNT for both adsorption and desorption stages of the selected HeCol cycle. The commercial

Maxsorb III is available in the form of fine powder with the particle size  $< 10 \mu\text{m}$ , which could not be directly used for dynamic testing. Therefore, the powder is shaped to larger particles by either using a binder (polyvinyl alcohol, PVA) or pressing (Section 2). Their textural characteristics were studied by a low-temperature nitrogen adsorption.

## 2. Experimental

### 2.1. Samples Preparation

#### Consolidation of the Carbon Maxsorb III Powder

The activated carbon Maxsorb III (Kensi Coke and Chemicals Co. Ltd., Osaka, Japan) was chosen in this paper for the detailed study of methanol adsorption. The carbon grains were prepared from the Maxsorb III powder by using PVA as a binder. In this process, 0.5 g of the carbon was mixed with 0.28 or 0.44 g of 20 wt.% PVA aqueous solution to get pastes P1 and P2, respectively. The obtained pastes were dried at room temperature for 16 h and then at  $120 \text{ }^\circ\text{C}$  for 2 h. The solid residues were ground and sieved to get grains with a size of 1.6–1.8 mm (samples S(P1)120 and S(P2)120). The grains were calcined in the argon flow at  $400 \text{ }^\circ\text{C}$  for 4 h to carbonize PVA (samples S(P1)400 and S(P2)400). A part of paste P1 was pressed at 10 atm, dried at room temperature, dried again at  $120 \text{ }^\circ\text{C}$ , ground and sieved (sample SP(P1)120). A low-temperature nitrogen adsorption analyzer Quantachrome Nova 1200e was used to study the texture characteristics of the samples (experimental data are presented in the supplementary materials: Figures S1–S4 and Tables S1–S4). The specific pore volume was calculated from nitrogen adsorption at  $P/P_0 = 0.99$ , by using the BJH method (desorption branch), the specific surface area was calculated using BET analysis.

Activated carbon ACM-35.4 with the average pore size  $d_{\text{av}} = 2.3 \text{ nm}$ , the specific surface area  $S_{\text{sp}} = 1200 \text{ m}^2/\text{g}$ , and the specific pore volume  $V_p = 0.69 \text{ cm}^3/\text{g}$  produced by the CECA Arkema group was milled and sieved to get the required fraction of 1.6–1.8 mm.

The composite LiCl (34 wt.%)/MWCNT was prepared according to the procedure, described in [20]. The grains of 1.6–1.8 mm size were studied.

### 2.2. Experimental Study of Methanol Ad/Desorption Dynamics

The dynamic experiments were performed for two quite different HeCol cycles under the same boundary conditions as in reference [21]: the boundary temperatures  $T_L/T_M/T_H = -30/2/30 \text{ }^\circ\text{C}$  (Figure 1b). Appropriate boundary pressures are as follows:  $P_1 = P_0(T_L) = 4.7 \text{ mbar}$ , that is the saturated methanol pressure at  $T_L = -30 \text{ }^\circ\text{C}$ ,  $P_2 = 26.8 \text{ mbar}$ ,  $P_3 = P_0(T_M) = 45.1 \text{ mbar}$ , that is the saturated methanol pressure at  $T_M = 2 \text{ }^\circ\text{C}$ , and  $P_4 = 8.2 \text{ mbar}$ . The corresponding methanol uptakes are obtained from the equilibrium adsorption data taken from the literature for Maxsorb III [22] and LiCl (34 wt.%)/MWCNT [17] (Table 1).

Isothermal dynamics of the methanol ad/desorption was studied by means of an experimental test rig described in [21]. The rig consists of the three main parts: a measuring cell loaded with the studied adsorbent, a buffering vessel, and a condenser/evaporator with liquid methanol. Loose adsorbent grains were placed on metal support in one layer. The adsorbent mass  $m_a$  was ca. 50 mg for both the carbon and composite. The temperature of metal support was maintained as constant and equal to  $T_H = 30 \text{ }^\circ\text{C}$  and  $T_M = 2 \text{ }^\circ\text{C}$  during the adsorption and desorption runs, respectively. The adsorption process (stage 2–3 in Figure 1) was initiated by the rapid increase in the methanol vapor pressure over the adsorbent; the measuring cell was filled with methanol vapor from the evaporator to reach the initial adsorption pressure  $P_2 = 26.8 \text{ mbar}$ . At the same time, the adsorbent temperature was fixed at  $T_2 = T_H = 30 \text{ }^\circ\text{C}$ . After setting the adsorption equilibrium at point 2 (the uptake  $w_1 = w(T_2, P_2)$ ), the measuring cell was disconnected from the evaporator and connected to the buffering vessel with the initial methanol pressure 46.4 mbar. This initiated the methanol adsorption, which resulted in a gradual decrease in its pressure  $P(t)$  to the final (equilibrium) pressure,  $P_3 = 45.1 \text{ mbar}$ . Desorption

runs were performed in a similar way by a drop of the methanol vapor pressure (stage 4–1 in Figure 1) with the initial pressure,  $P_4 = 8.2$  mbar, and the final pressure,  $P_1 = 4.7$  mbar, at  $T_1 = T_M = 2$  °C.

**Table 1.** Texture characteristics of the studied carbons and specific mass of methanol exchanged in the HeCol cycles analyzed.

AC	$V_{sp}$ , cm <sup>3</sup> /g	$S_{sp}$ , m <sup>2</sup> /g	$\rho$ , g/cm <sup>3</sup>	Cycle 1	Cycle 2	Reference
				$\Delta w$ , g/g (g/cm <sup>3</sup> )		
MaxSorb III	1.72	3150	0.17	0.82 (0.14)	0.24 (0.041)	[9]
SRD1352/3	0.82	2610	0.42	0.40 (0.17)	0.18 (0.076)	[5]
ACM-35.4	0.69	1200	0.4	0.23 (0.09)	0.08 (0.033)	[23]
Sibunit	0.86	450	0.4	0.10 (0.04)	0.03 (0.012)	[3]
G32-H	0.48	920	0.37	0.13 (0.05)	0.07 (0.026)	[5]
Norit RX 3 Extra	0.55	1000	0.38	0.19 (0.07)	0.09 (0.034)	[5]
Norit R 1 Extra	0.52	1050	0.42	0.20 (0.08)	0.10 (0.042)	[5]
Ruthers CG1-3	0.54	1010	0.37	0.17 (0.06)	0.09 (0.033)	[5]
AquaSorb2000	1.04	1050	0.48	0.45 (0.22)	-	[24]
HDACF	1.70 <sup>1</sup>	3260 <sup>1</sup>	0.36	0.8 (0.30)	0.25 (0.10)	[25]
CarboTech C40/1	0.63	1290	0.38	0.36 (0.14)	0.12 (0.046)	[5]
CarboTech A35/1	0.79	1410	0.33	0.44 (0.15)	0.15 (0.050)	[5]
LiCl (34%)/MWCNT	1.40	140	0.23	1.27 (0.29)	0.62 (0.14)	[17]

<sup>1</sup> For virgin (not pressed) HDACF.

The pressure change was recorded every 1 s by an absolute pressure transducer Barocel™ 600 with an accuracy of ±0.15%. The experimental pressure evolution  $P(t)$  was used to calculate the methanol uptake/release  $w(t)$  and the dimensionless conversion  $\chi = (P(t) - P(t = 0))/(P(t \rightarrow \infty) - P(t = 0))$ . The accumulated error in the absolute methanol loading was  $\pm 10^{-3}$  g/g, leading to the accuracy of the differential methanol loading  $w(t)$  equal to ±3%.

### 3. Comparative Analysis of Activated Carbons in the HeCol Cycle

In this section, we make a comparison of various commercial and innovative ACs as methanol adsorbents for the HeCol cycle. Available equilibrium data on the methanol vapor adsorption on the ACs are taken from the literature [5,19,23–26]. The useful heat  $Q_{us}$  per cycle is the main output parameter of any HeCol cycle [9]. It depends on the specific mass of methanol  $\Delta w$  exchanged in the cycle. The values  $\Delta w$  and  $Q_{us}$  are assessed to choose carbons, which are the most promising for typical HeCol cycles. A brief comparison with the carbonaceous composite LiCl/MWCNT is also made.

#### 3.1. Specific Mass of Methanol Exchanged

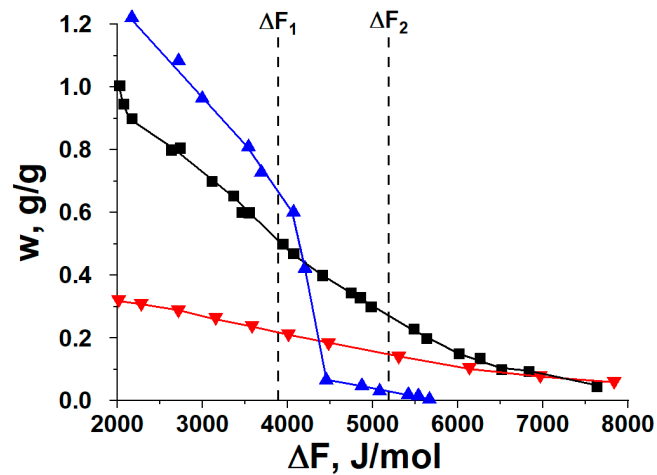
The literature adsorption data for working pairs “methanol—AC” are analysed for two quite different HeCol cycles. Cycle 1, with the boundary temperatures  $T_L/T_M/T_H = -20/20/35$  °C, is easier for implementation, and cycle 2, with  $T_L/T_M/T_H = -30/2/30$  °C, is more difficult (Figure 1b). This analysis aimed at evaluating the specific mass of methanol  $\Delta w$  exchanged in these cycles (Table 1).

Table 1 shows that the methanol exchange for cycle 1 is 2–4 times larger than for cycle 2, which is because the latter cycle is narrower in the  $P$ - $T$  presentation (Figure 1b). Carbon Maxsorb III exhibits a maximum methanol exchange for both cycles:  $\Delta w = 0.82$  and  $0.24$  g/g, respectively. It is 3–3.5 times larger than for carbon ACM-35.4 tested in the first HeCol prototype [12]. For cycle 1, quite large methanol exchange (0.17–0.44 g/g) is found for other ACs with the specific surface area larger than 1000 m<sup>2</sup>/g (Table 2). At lower condensation temperature ( $T_L = -30$  °C),  $\Delta w$  increases to 0.26–0.47 g/g

(not presented). This confirms that the HeCol cycle better operates at colder ambient temperature. Table 1 shows that the composite LiCl/MWCNT exchanges more methanol even compared with the best carbon (Maxsorb III). This is especially pronounced for cycle 2 (0.62 g/g instead of 0.24 g/g). This is due to the very steep and properly positioned universal curve of methanol sorption (Figure 2). Moreover, almost the same mass of methanol is exchanged at the adsorption potential  $\Delta F_2 = -R \cdot T_M \cdot \ln(P_L/P_M) = 4500$  J/mol instead of 5200 J/mol for cycle 2. This means that at  $T_M = 2$  °C, the ambient temperature  $T_L = -26$  °C is sufficient for regeneration instead of  $-30$  °C.

**Table 2.** Specific heat capacity  $C$  of inert components of the analyzed adsorbent–heat exchanger (AdHEX).

Component	$C$ , J/kg K	Reference
Aluminium	903	[27]
Methanol	2490	[27]
Coal	740	[28]
Lithium Chloride	1130	[29]



**Figure 2.** Equilibrium adsorption of methanol on MaxSorb III (■), LiCl confined to multi-wall carbon nanotubes (LiCl (34 wt.)/MWCNT) (▲), and ACM-35 (▼) as a function of the free adsorption energy  $\Delta F$ . The dashed lines represent the adsorption potential corresponding to the rich ( $\Delta F_1 = 3900$  J/mol) and weak ( $\Delta F_2 = 5200$  J/mol) isosteres of the HeCol cycle with the boundary temperatures  $T_L/T_M/T_H = -30/2/30$  °C.

The exchanged specific mass of methanol  $\Delta w$  displayed in Table 1 is used in the next section to evaluate the main output parameter of the HeCol cycle that is the specific useful heat. It is worth mentioning that the apparent density of the carbons involved and the composite LiCl/MWCNT is quite low (0.17–0.48 g/cm<sup>3</sup>). Therefore, the methanol exchange related to a unit volume is modest, e.g., 0.14 and 0.29 g/cm<sup>3</sup> for Maxsorb III and LiCl/MWCNT, respectively. This is because the carbons are available mainly as a fine powder, fibers, etc. The conventional way to increase the density by a factor of 1.5–3.0 is their compaction in a denser structure [7]. We have performed such compaction by using the binder (see Section 2.1).

### 3.2. Specific Useful Heat

Here, we evaluate the performances of typical HeCol cycle in terms of the specific useful heat  $Q_{us}$  [J/g-adsorbent] per cycle. It is equal to the adsorption heat  $Q_{ads}$  released at stage 2–3 excluding the sensible heat  $Q_{sen}$  consumed at stage 1–2 related to the adsorbent mass  $m_a$

$$Q_{us} = (Q_{ads} - Q_{sen})/m_a = \Delta H_{ads}\Delta w - CM(T_H - T_M)/m_a, \quad (1)$$

where  $\Delta H_{ads}$  is the specific adsorption heat [J/g-methanol],  $C$  and  $M$  are the overall specific heat capacity and mass of inert components, and  $T_H$  and  $T_M$  are the temperatures of adsorption and regeneration (Figure 1a). The specific heat of methanol in the gas phase is neglected since its mass is much smaller than that in the adsorbed state [10]. The overall specific heat capacity  $C$  and mass  $M$  of inert components concern adsorbent, adsorbate, and metal heat exchanger which together make up an “adsorbent–heat exchanger” (AdHEX). Equation (1) predicts that there exists a threshold exchange  $\Delta w^* = [C \cdot M \cdot (T_H - T_M)] / (\Delta H_{ads} \cdot m_a)$  at which the adsorption heat equals the sensible heat, so that there is no useful effect.

The specific useful heat is evaluated for the HeCol prototype [15] loaded with two carbonaceous adsorbents, namely, carbon Maxsorb III and the composite LiCl (34%)/MWCNT [18]. This HEX consists of a plate-tube finned heat exchanger (Yamaha Aerox) made of aluminum with the dimensions  $190 \times 200 \times 30 \text{ mm}^3$  ( $M_{Al} = 0.50 \text{ kg}$ ). The adsorbent mass  $m_a$  is 0.15 and 0.25 kg for the AC and the composite, respectively. The specific adsorption heat  $\Delta H_{ads}$  is  $(1.30 \pm 0.20)$  and  $(1.41 \pm 0.07) \text{ kJ/g}$  for Maxsorb III [22] and LiCl/MWCNT [17]. Equation (1) can be re-written as

$$Q_{us} = Q_{ads} - (Q_{sen}^{adsorbent} + Q_{sen}^{adsorbate} + Q_{sen}^{metal}) = \Delta H_{ads} \Delta w - [C_{LiCl} \omega_{LiCl} + C_{coal} (1 - \omega_{LiCl}) + C_{methanol} w_1 + C_{Al} M_{Al} / m_a] (T_H - T_M) \tag{2}$$

where  $\omega_{LiCl}$  is the salt mass fraction in the adsorbent (0 for the carbon and 0.34 for the composite),  $w_1$  is the methanol content corresponding to weak isostere (1–2). The specific heat capacity  $C$  of inert components is presented in Table 2.

The useful heat is generated only if  $\Delta w > \Delta w^* = 0.052$  and  $0.032 \text{ g/g}$  for the AC and the composite, respectively (Figure 3). To obtain a reasonable  $Q_{us}$ -value of  $500 \text{ J/g}$ , it is needed to exchange  $0.44$  and  $0.39 \text{ g-methanol/g}$  for Maxsorb III and the composite that can be reached for cycle 1. So large exchange is also possible when carbons SRD1352/3 and CarboTech A35/1 are used (Table 1). Maximum specific useful heat amounting to  $990$  and  $1750 \text{ J/g}$  can be obtained for Maxsorb III and LiCl/MWCNT, respectively (Figure 3). On the contrary, no one adsorbent among those tested here is suitable for cycle 2, and advanced materials and adsorptives are welcome.

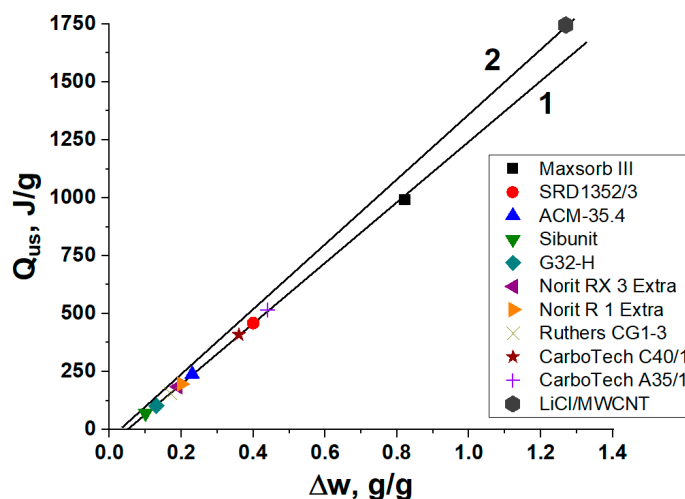


**Figure 3.** Useful heat of various activated carbons (1) and composite LiCl/MWCNT (2) for cycle 1 (see details in the text).

#### 4. Dynamics of Methanol Ad/Desorption

Carbon Maxsorb III ensures the best thermodynamic performance in the HeCol cycle among the tested carbons. Even larger methanol exchange and useful heat can be obtained for the composite LiCl/MWCNT (Figure 3). For this reason, these two sorbents are used for experimental study of the HeCol dynamics. Namely, slow desorption at low temperature and pressure can be a big problem

on the way to the HeCol practical implementation [21,30]. For the sake of comparison, the dynamic experiments are performed under the same conditions as in ref. [21] for ACM-35.4. The appropriate temperatures and pressures are displayed in Table 3 ( $P_o = P_2$  for adsorption and  $P_4$  for desorption;  $P_f = P_3$  for adsorption and  $P_1$  for desorption).

**Table 3.** Boundary temperature, initial  $P_o$  and final  $P_f$  pressures for the dynamic measurements.

Conditions	$T, ^\circ\text{C}$	$P_o, \text{mbar}$	$P_f, \text{mbar}$
Adsorption	30	26.8	45.1
Desorption	2	8.2	4.7

#### 4.1. Texture of the Compacted Maxsorb III Samples

As mentioned in the Introduction, the original Maxsorb III powder could not be directly used for dynamic tests. Therefore, it was compacted to larger particles as described in Section 2, and the textural characteristics of the prepared samples are studied by the low-temperature nitrogen adsorption. Both the pore volume and surface area of the samples are smaller than those of the Maxsorb III powder by a factor of 1.12–1.26 (Table 4). This is somewhat larger than the increase in the sample mass due to the addition of the inert binder. This may indicate a slight blockage of the pore surface and volume as a result of the carbon compaction. Both values still remain sufficient to ensure the large methanol uptake. Indeed, the specific mass of methanol exchanged in cycle 2 is only slightly smaller than for the non-treated Maxsorb III (the last column in Table 4).

**Table 4.** Specific pore volume  $V_{sp}$  and surface area  $S_{sp}$ , binder content  $B$ , and methanol exchange  $\Delta w$  (cycle 2) during the dynamic tests for the compacted MaxSorb III samples.

Sample	$V_{sp}, \text{cm}^3/\text{g}$	$S_{sp}, \text{m}^2/\text{g}$	$B, \text{wt. } \%$	$\Delta w, \text{g/g}$
MaxSorb-III	1.72	3150	0	0.24
S(P1)120	1.37	2605	10	0.19
SP(P1)120	1.43	2710	10	0.20
S(P1)400	1.53	2880	<10	0.22
S(P2)400	1.51	2895	<10	0.22

#### 4.2. Adsorption and Desorption Kinetics

An initial part of the all kinetic curves can be described by the exponential equation:

$$\chi = 1 - \exp(-t/\tau) \quad (3)$$

up to the dimensionless conversion ( $\chi \leq 0.6$ – $0.9$ ) (Figure 4). The exponential time  $\tau$  is displayed in Table 5. For all samples prepared, desorption is slower than adsorption. This is probably due to the fact that desorption occurs at a lower temperature ( $2^\circ\text{C}$ ) and is initiated by a small drop in the methanol pressure,  $\Delta P = 8.2 \text{ mbar} - 4.7 \text{ mbar} = 3.5 \text{ mbar}$  (Table 3). The initial adsorption and desorption rates, which are proportional to  $(1/\tau)$ , differ by a factor of 1.6 or less. At  $\chi > 0.6$ – $0.9$ , both processes become slower than Equation (3) predicts, and can be characterized by the characteristic times  $\tau_{0.7}$  and  $\tau_{0.8}$ , which correspond to  $\chi = 0.7$  and  $0.8$  (Table 5).

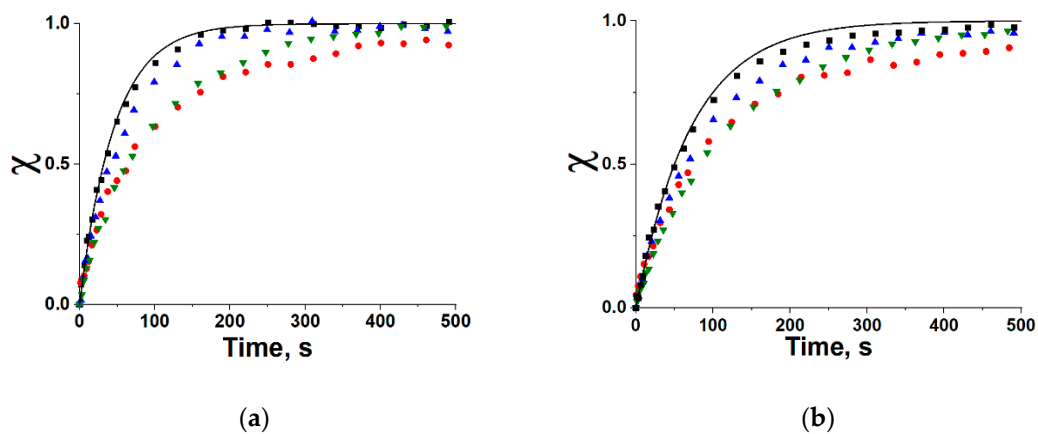


**Figure 4.** Dimensionless methanol uptake (a) and release (b) curves for the compacted MaxSorb samples: S(P1)400 (■), S(P1)120 (●), SP(P1)120 (▲), S(P2)400 (▼). Solid lines give an example of exponential approximation (3).

At small conversions ( $\chi < 0.2$ ), there is only a small difference between the compacted samples that may indicate the same dominant dynamic resistance. As at the short time, the driving force for mass transfer is maximal [31], the limiting process could be heat transfer between the carbon grains and the metal support. The sorption dynamics for the consolidated Maxsorb samples differ significantly at larger  $\chi$  (Figure 4), which can be explained by increasing the contribution of mass transfer resistance to the sorption rate. In this case, the difference in the sample’s texture (Table 4) begins to affect the dynamics. At any time, the fastest adsorption and desorption are found for sample S(P1)400 calcined at  $T = 400$  °C. Pressed sample SP(P1)120 demonstrates only slightly slower dynamics. For S(P2)400 with the higher binder content, both processes are slower by a factor of 1.6–1.9. Sample S(P1)120, prepared by simple drying of paste P1 at 120 °C, demonstrates the slowest process. However, even for the worst sample, significant conversion of 0.7 is reached for 190–225 s, corresponding to a quite promising value of the specific power  $W_{0.8} \approx 1$  kW/kg (Table 5, see details in Section 4.3).

**Table 5.** Characteristic times  $\tau$ ,  $\tau_{0.7}$ ,  $\tau_{0.8}$  and specific powers  $W_{max}$ ,  $W_{0.7}$ , and  $W_{0.8}$  for the prepared Maxsorb III samples, ACM-35.4, and LiCl/MWCNT (cycle –30/2/30 °C).

Sample	Runs	$\tau$ , s	$\tau_{0.7}$ , s	$\tau_{0.8}$ , s	$W_{max}$ , kW/kg	$W_{0.7}$ , kW/kg	$W_{0.8}$ , kW/kg
S(P1)400	Ads	46	60	80	6.2	3.3	2.8
	Des	72	93	127	4.0	2.1	1.8
SP(P1)120	Ads	58	76	103	4.5	2.4	2.0
	Des	88	121	164	2.9	1.5	1.3
S(P1)120	Ads	74	129	188	3.3	1.3	1.0
	Des	102	151	225	2.4	1.1	0.9
S(P2)400	Ads	88	117	163	3.2	1.7	1.4
	Des	115	153	215	2.5	1.3	1.1
ACM-53.4	Ads <sup>1</sup>	54	85	125	1.7	0.8	0.6
	Des <sup>2</sup>	76	94	-	1.3	0.7	-
LiCl/MWCNT	Ads	390	476	625	2.2	1.3	1.1
	Des	460	1180	1560	1.9	0.5	0.4

<sup>1</sup> measured in this work. <sup>2</sup> taken from [21].

The adsorption and desorption of methanol for sample S(P1)400 are significantly faster than for ACM-35.4 and LiCl/MWCNT in terms of both initial sorption rate (Figure 5) and exponential time (Table 5). This material is the best from the dynamic point of view.

The initial rate of methanol sorption on LiCl/MWCNT is much smaller than for Maxsorb III. Moreover, a strong slowing down is observed for desorption at  $t > 200$  s so that the equilibrium exchange ( $\Delta w = 0.62$  g/g) is not reached, even for 2000 s (Figure 5). The release curve can be decomposed into slow and fast components (Figure 6a) in two ways giving the same accuracy. The first presentation corresponds to two parallel processes described by exponentials  $\Delta w(t) = 0.06$  g/g $\cdot$ [1 - exp(- $t/\tau_1$ )] + 0.56 g/g $\cdot$ [1 - exp(- $t/\tau_2$ )] with  $\tau_1 = 510$  s and  $\tau_2 = 1070$  s. The second one assumes two sequential processes and gives the following expression:  $\Delta w(t) = 0.21$  g/g $\cdot$ [1 - exp(- $t/\tau_1$ )] + 0.41 g/g $\cdot$ [1 - exp(-( $t - 365$ s)/ $\tau_2$ )] with  $\tau_1 = 150$  s and  $\tau_2 = 1050$  s. Both equations can be used by an interested reader for mathematical modeling of the desorption dynamics.

The fast desorption is probably associated with methanol removal from the solution confined to the sample pores ( $\Delta w \leq 0.10$  g/g). The slow process can be due to the decomposition reaction  $\text{LiCl}\cdot 3\text{CH}_3\text{OH} = \text{LiCl} + 3\text{CH}_3\text{OH}$  [23]. Indeed, many gas–solid reactions are kinetically hindered, and thermally activated reconstruction of a crystalline lattice is necessary [32]. Moreover, desorption can be decelerated by slow heterogeneous nucleation of the salt on the matrix surface and a sluggish formation of crystalline solvates or salt. Such kinetics cannot be described by a single exponential equation, which is more applicable for simpler systems, therefore, two-exponential approximations were considered.

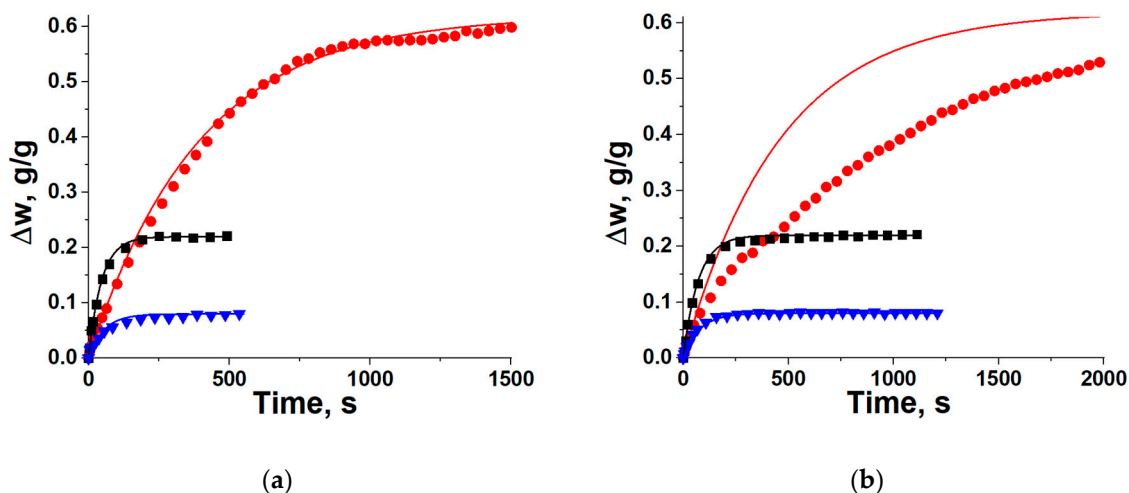


**Figure 5.** Methanol uptake (a) and release (b) curves for Maxsorb III S(P1)400 (■), ACM-35.4 (▼), and LiCl/MWCNT (●). Solid lines—exponential approximation (3).

For this reason, we have performed experiments on the methanol desorption at higher  $T_M = 6$  and  $10$  °C. Under these more favorable conditions, the methanol exchange greatly increases (to 0.87 and 1.08 g/g, respectively) and desorption gets much faster (Figure 6b and Table 6). These great exchanges lead to the large useful heat  $Q_{us} = 1160$  and 1460 J/g (Figure 3). It demonstrates that the effect of desorption/evaporation temperature  $T_M$  on both thermodynamic and dynamic outputs of HeCol cycles is strong. In fact, the composite LiCl/MWCNT can hardly be used at  $T_M = 2$  °C, because of the slow and incomplete desorption. However, it is very promising from both the thermodynamic and dynamic points of view at  $T_M \geq 6$  °C.

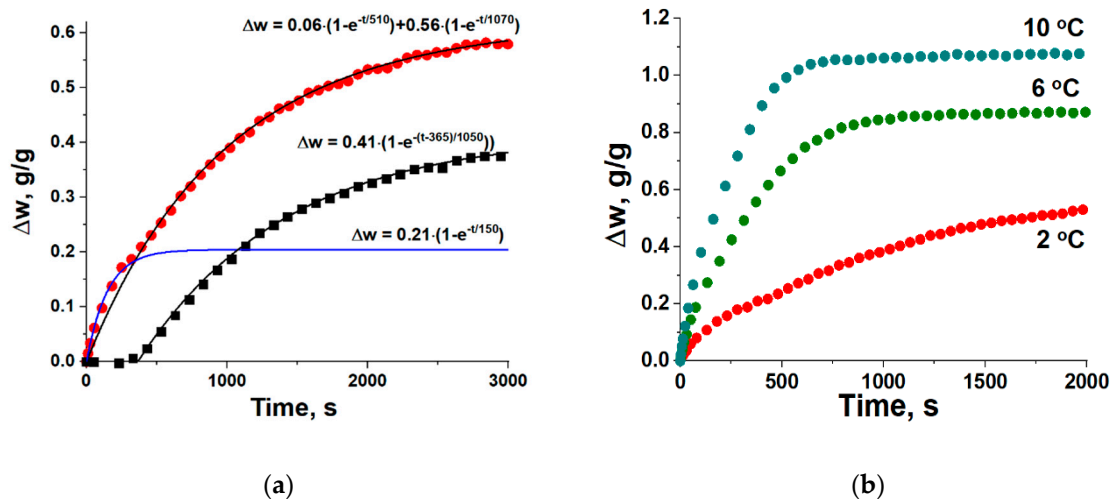


**Figure 6.** (a) Fast and slow components of methanol release curve at  $T_M = 2\text{ }^\circ\text{C}$ ; (b) methanol release curves measured at various  $T_M$  listed near the curves. Composite LiCl/MWCNT.

**Table 6.** Characteristic times  $\tau$ ,  $\tau_{0.7}$ ,  $\tau_{0.8}$  and specific powers  $W_{\max}$ ,  $W_{0.7}$ , and  $W_{0.8}$  for methanol desorption from LiCl/MWCNT (cycle  $-30/T_M/30\text{ }^\circ\text{C}$ ) at various desorption temperature  $T_M$ .

$T_M, \text{ }^\circ\text{C}$	$\tau, \text{ s}$	$\tau_{0.7}, \text{ s}$	$\tau_{0.8}, \text{ s}$	$W_{\max}, \text{ kW/kg}$	$W_{0.7}, \text{ kW/kg}$	$W_{0.8}, \text{ kW/kg}$
2	460	1180	1560	1.9	0.5	0.4
6	290	425	535	4.2	2.0	1.8
10	200	300	375	7.6	3.6	3.2

### 4.3. Specific Power at Adsorption and Desorption Stages

The maximal specific power  $W_{\max}$  generated by or supplied to adsorbent during desorption or adsorption runs is the main dynamic indicator of any HeCol process. It can be calculated using the experimentally measured exponential time (Table 5):

$$W_{\max} = \Delta w \cdot \Delta H_{\text{ads}} / \tau, \tag{4}$$

where  $\Delta H_{\text{ads}} = (1.30 \pm 0.20)$  kJ/g for the carbons and  $(1.41 \pm 0.07)$  kJ/g for the composite. At long times, the average specific powers  $W_{0.7}$  и  $W_{0.8}$  are characterized by the time  $\tau_\chi = \tau_{0.7}$  or  $\tau_{0.8}$  (Tables 5 and 6):

$$W_\chi = \chi \cdot \Delta w \cdot \Delta H_{\text{ads}} / \tau_\chi, \tag{5}$$

Under conditions of the more harsh cycle with the boundary temperatures  $-30/2/30\text{ }^\circ\text{C}$ , the  $W_{\max}$ -value reaches 6.2 and 4.0 kW/(kg-Maxsorb S(P1)400), which could be very promising for implementation of the HeCol cycle in compact AdHex units. The more practical value  $W_{0.7}$  (3.3 kW/kg) is also quite reasonable. About three times smaller powers can be obtained by using the composite LiCl/MWCNT (Table 5). However, the methanol desorption from this sorbent becomes significantly faster at  $T_M \geq 6\text{ }^\circ\text{C}$ , so that the maximum power reaches 4–8 kW/kg (Table 6).

## 5. Summary

Porous carbonaceous materials have been well known since ancient times, when wood chars were used in medicine, water purification and the manufacture of bronze. In this day, many commercial activated carbons (ACs) are widely used in various adsorption technologies, including adsorptive heat transformation and storage (AHTS). This work addresses the applicability of commercial ACs and an innovative carbonaceous composite “LiCl in multi-wall carbon nanotubes” (LiCl/MWCNT) in a new cycle “Heat from Cold” (HeCol). This cycle proposed for the amplification of low-temperature

ambient heat in cold countries was analyzed with methanol as an adsorptive and a commercial carbon ACM-35.4 as an adsorbent. These studies demonstrated that the HeCol cycle is feasible; however, carbons with a larger mass of methanol exchanged in the HeCol cycle are welcome.

The useful heat generated per cycle is the main performance indicator of HeCol cycles. It can reach 990 and 1750 J/g by using the carbon Maxsorb III and the composite, respectively, which is much larger than for ACM-35.4. For these materials, methanol adsorption dynamics under typical conditions of HeCol cycles is experimentally studied by the large pressure jump method. Before making this analysis, the fine carbon powder is consolidated by using a binder (polyvinyl alcohol) or pressing to obtain larger particles (ca. 2 mm). The methanol desorption at  $T = 2\text{ }^{\circ}\text{C}$  from the consolidated samples of Maxsorb III is faster than for LiCl/MWCNT, and the maximum (initial) useful power reaches (2.5–4.0) kW/kg-carbon. It is promising for designing compact HeCol units utilizing this carbon. It is worth mentioning that Maxsorb III is also very capable of adsorbing ammonia and hydrofluorocarbons (R32, R134, R152), which can be considered as alternative adsorptives for HeCol cycles [33].

This study emphasizes the promise of activated carbons for application in the new adsorptive cycle “Heat from Cold” and highlights that the carbon Maxsorb III is the most promising from both thermodynamic and kinetic points of view.

**Supplementary Materials:** The following are available online at <http://www.mdpi.com/2079-6439/8/8/51/s1>, Figure S1: Isotherm of nitrogen adsorption on S(P1)120, Figure S2: Isotherm of nitrogen adsorption on S(P1)400, Figure S3: Isotherm of nitrogen adsorption on S(P2)400, Figure S4: Isotherm of nitrogen adsorption on SP(P1)120, Table S1: Experimental data of nitrogen adsorption on S(P1)120, Table S2: Experimental data of nitrogen adsorption on S(P1)400, Table S3: Experimental data of nitrogen adsorption on S(P2)400, Table S4: Experimental data of nitrogen adsorption on SP(P1)120.

**Author Contributions:** Conceptualization, Y.A.; methodology, Y.A.; validation, I.G., A.G., L.G. and Y.A.; formal analysis, I.G., L.G. and Y.A.; investigation, I.G. and A.G.; resources, A.G.; data curation, I.G., A.G. and L.G.; writing—original draft preparation, Y.A.; writing—review and editing, I.G., A.G. and L.G.; visualization, I.G. and A.G.; supervision, Y.A.; project administration, Y.A.; funding acquisition, Y.A. All authors have read and agreed to the published version of the manuscript.

**Funding:** This work was supported by the Russian Science Foundation (grant N 16-19-10259).

**Acknowledgments:** The authors thank B.B. Saha for providing us with Maxsorb III powder.

**Conflicts of Interest:** The authors declare no conflict of interest.

## Nomenclature

$B$	binder content, wt. %
$C$	specific heat capacity, J/(g K)
$F$	adsorption potential, J/mol
$H$	enthalpy, J/mol
$M, m$	mass, g
$P$	pressure, mbar
$Q$	specific heat, J/g
$R$	universal gas constant, 8.314 J/(K mol)
$S_{sp}$	specific surface area, $\text{m}^2/\text{g}$
$T$	temperature, K, $^{\circ}\text{C}$
$t$	time, s
$V_{sp}$	specific pore volume, $\text{cm}^3/\text{g}$
$W$	specific power, W/g
$w$	specific adsorbate mass, g/g
wt.%	weight %

## Greek Symbols

$\tau$	characteristic time, s
$\rho$	density, g/cm <sup>3</sup>
$\chi$	dimensionless conversion, dimensionless
$\omega$	salt mass fraction, dimensionless

## Subscript

0.7	70% conversion
0.8	80% conversion
a	adsorbent
ads	adsorption
Al	aluminum
con	condensation
des	desorption
ev	evaporation
f	final
H	high
L	low
LiCl	lithium chloride
M	medium
max	maximal
o	initial
sen	sensible
us	useful

## Abbreviation

3T	three temperature
AdHex	Adsorbent—heat exchanger
AC	activated carbon
AHTS	adsorptive heat transformation and storage
HeCol	Heat from Cold
HEX	heat exchanger
HDACF	high density activated carbon fiber
MWCNT	Multi-wall carbon nanotubes

## References

1. Joachim, H. *Papyrus Ebers*; de Gruyter: Berlin, Germany, 1890.
2. Schueth, F.; Sing, K.S.W.; Weitkamp, J. *Handbook of Porous Solids Vol. 1 and 3*; Willey-VCH: Weinheim, Germany, 2002.
3. Yang, R.T. *Adsorbents: Fundamentals and Applications*; John Wiley & Sons, Inc.: Hoboken, NJ, USA, 2003.
4. Kostoglou, N.; Koczwara, C.; Prehal, C.; Terziyska, V.; Babic, B.; Matovic, B.; Constantinides, G.; Tampaxis, C.; Charalambopoulou, G.; Steriotis, T.; et al. Nanoporous activated carbon cloth as a versatile material for hydrogen adsorption, selective gas separation and electrochemical energy storage. *Nano Energy* **2017**, *40*, 49–64. [[CrossRef](#)]
5. Henninger, S.; Schicktanz, M.; Hügenell, P.; Sievers, H.; Henning, H.-M. Evaluation of methanol adsorption on activated carbons for thermally driven chillers part I: Thermophysical characterisation. *Int. J. Refrig.* **2012**, *35*, 543–553. [[CrossRef](#)]
6. Freni, A.; Maggio, G.; Sapienza, A.; Frazzica, A.; Restuccia, G.; Vasta, S. Comparative analysis of promising adsorbent/adsorbate pairs for adsorptive heat pumping, air conditioning and refrigeration. *Appl. Therm. Eng.* **2016**, *104*, 85–95. [[CrossRef](#)]

7. Boubakri, A.; Arsalane, M.; Yous, B.; Ali-Moussa, L.; Pons, M.; Meunier, F.; Guillemot, J. Experimental study of adsorptive solar-powered ice makers in Agadir (Morocco)—2. Influences of meteorological parameters. *Renew. Energy* **1992**, *2*, 15–21. [[CrossRef](#)]
8. Pal, A.; Uddin, K.; Thu, K.; Saha, B.B. Activated carbon and graphene nanoplatelets based novel composite for performance enhancement of adsorption cooling cycle. *Energy Convers. Manag.* **2019**, *180*, 134–148. [[CrossRef](#)]
9. Aristov, Y. Adsorptive transformation of ambient heat: A new cycle. *Appl. Therm. Eng.* **2017**, *124*, 521–524. [[CrossRef](#)]
10. Okunev, B.N.; Voskresensky, N.M.; Girmik, I.S.; Aristov, Y. Thermodynamic Analysis of the New Adsorption Cycle “HeCol” for Ambient Heat Upgrading: Ideal Heat Transfer. *J. Eng. Thermophys.* **2018**, *27*, 327–338. [[CrossRef](#)]
11. Voskresenskii, N.M.; Okunev, B.N.; Gordeeva, L.G. A Thermodynamic Analysis of a New Cycle for Adsorption Heat Pump “Heat from Cold”: Effect of the Working Pair on Cycle Efficiency. *Therm. Eng.* **2018**, *65*, 524–530. [[CrossRef](#)]
12. Gordeeva, L.G.; Tokarev, M.M.; Aristov, Y. New Adsorption Cycle for Upgrading the Ambient Heat. *Theor. Found. Chem. Eng.* **2018**, *52*, 195–205. [[CrossRef](#)]
13. Tokarev, M.M.; Grekova, A.D.; Gordeeva, L.G.; Aristov, Y.I. A new cycle “Heat from Cold” for upgrading the ambient heat: The testing a lab-scale prototype with the composite sorbent CaClBr/silica. *Appl. Energy* **2018**, *211*, 136–145. [[CrossRef](#)]
14. Tokarev, M.; Gordeeva, L.G.; Shkatulov, A.; Aristov, Y.I. Testing the lab-scale “Heat from Cold” prototype with the “LiCl/silica—Methanol” working pair. *Energy Convers. Manag.* **2018**, *159*, 213–220. [[CrossRef](#)]
15. Tokarev, M. A Double-Bed Adsorptive Heat Transformer for Upgrading Ambient Heat: Design and First Tests. *Energies* **2019**, *12*, 4037. [[CrossRef](#)]
16. Pons, M.; Meunier, F.; Cacciola, G.; Critoph, R.; Groll, M.; Puigjaner, L.; Spinner, B.; Ziegler, F. Thermodynamic based comparison of sorption systems for cooling and heat pumping. *Int. J. Refrig.* **1999**, *22*, 5–17. [[CrossRef](#)]
17. Grekova, A.; Gordeeva, L.G.; Aristov, Y. Composite sorbents “Li/Ca halogenides inside Multi-wall Carbon Nano-tubes” for Thermal Energy Storage. *Sol. Energy Mater. Sol. Cells* **2016**, *155*, 176–183. [[CrossRef](#)]
18. Girmik, I.S.; Grekova, A.D.; Li, T.; Wang, R.; Dutta, P.; Murthy, S.S.; Aristov, Y.I. Composite “LiCl/MWCNT/PVA” for advanced thermal battery: Dynamics of methanol sorption. *Ren. Sust. Energy Rev.* **2020**, *123*, 109748. [[CrossRef](#)]
19. Otowa, T.; Tanibata, R.; Itoh, M. Production and adsorption characteristics of MAXSORB: High-surface-area active carbon. *Gas. Separ. Purific.* **1993**, *7*, 241–245. [[CrossRef](#)]
20. Brancato, V.; Gordeeva, L.G.; Grekova, A.D.; Sapienza, A.; Vasta, S.; Frazzica, A.; Aristov, Y. Water adsorption equilibrium and dynamics of LiCl/MWCNT/PVA composite for adsorptive heat storage. *Sol. Energy Mater. Sol. Cells* **2019**, *193*, 133–140. [[CrossRef](#)]
21. Girmik, I.; Aristov, Y. A HeCol cycle for upgrading the ambient heat: The dynamic verification of desorption stage. *Appl. Therm. Eng.* **2019**, *146*, 608–612. [[CrossRef](#)]
22. El-Sharkawy, I.I.; Hassan, M.; Saha, B.B.; Koyama, S.; Nasr, M. Study on adsorption of methanol onto carbon based adsorbents. *Int. J. Refrig.* **2009**, *32*, 1579–1586. [[CrossRef](#)]
23. Gordeeva, L.G.; Aristov, Y. Dynamic study of methanol adsorption on activated carbon ACM-35.4 for enhancing the specific cooling power of adsorptive chillers. *Appl. Energy* **2014**, *117*, 127–133. [[CrossRef](#)]
24. Attalla, M.; Sadek, S.; Ahmed, M.S.; Shafie, I.M.; Hassan, M. Experimental study of solar powered ice maker using adsorption pair of activated carbon and methanol. *Appl. Therm. Eng.* **2018**, *141*, 877–886. [[CrossRef](#)]
25. Kumita, M.; Yamawaki, N.; Shinohara, K.; Higashi, H.; Kodama, A.; Kobayashi, N.; Seto, T.; Otani, Y. Methanol adsorption behaviors of compression-molded activated carbon fiber with PTFE. *Int. J. Refrig.* **2018**, *94*, 127–135. [[CrossRef](#)]
26. Golovin, V.A.; Gribov, E.N.; Simonov, P.A.; Okunev, A.G.; Voropaev, I.N.; Kuznetsov, A.N.; Romanenko, A.V. Development of carbon supports with increased corrosion resistance for Pt/C catalysts for oxygen electroreduction. *Kinet. Catal.* **2015**, *56*, 509–514. [[CrossRef](#)]
27. Lide, D.R. *Handbook of Chemistry and Physics*, 84th ed.; CRC: Boca Raton, FL, USA, 2004.
28. Rocky, K.A.; Islam, A.; Pal, A.; Ghosh, S.; Thu, K.; Saha, B.B. Experimental investigation of the specific heat capacity of parent materials and composite adsorbents for adsorption heat pumps. *Appl. Therm. Eng.* **2020**, *164*, 114431. [[CrossRef](#)]

29. Rabinovich, V.A.; Khavin, Z.Y. *Brief Chemical Reference Book*; Leningrad: Chemistry: St. Petersburg, Russia, 1977.
30. Aristov, Y. A new adsorptive cycle “HeCol” for upgrading the ambient heat: The current state of the art. *Int. J. Refrig.* **2019**, *105*, 19–32. [[CrossRef](#)]
31. Girnuk, I.S.; Okunev, B.N.; Aristov, Y.I. Dynamics of Pressure- and Temperature-Initiated Cycles for Upgrading Low Temperature Heat: Flat Bed of Loose Grains. *Appl. Therm. Eng.* **2020**, *165*, 114654. [[CrossRef](#)]
32. Galwey, A.; Brown, M. *Thermal Decomposition of Ionic Solids*; Elsevier Science: Amsterdam, The Netherlands, 1999.
33. Girnuk, I.; Tokarev, M.; Aristov, Y. Thermodynamic Analysis of Working Fluids for a New “Heat from Cold” Cycle. *Entropy* **2020**, *22*, 808. [[CrossRef](#)]



© 2020 by the authors. Licensee MDPI, Basel, Switzerland. This article is an open access article distributed under the terms and conditions of the Creative Commons Attribution (CC BY) license (<http://creativecommons.org/licenses/by/4.0/>).